Journal of Molecular Catalysis A: Chemical 304 (2009) 47–51

Contents lists available at ScienceDirect

Journal of Molecular Catalysis A: Chemical

journal homepage: www.elsevier.com/locate/molcata

Fischer–Tropsch synthesis on CaO-promoted Co/Al_2O_3 catalysts

Agudamu Bao, Kongyong Liew, Jinlin Li*

Key Laboratory of Catalysis and Materials Science of the State Ethnic Affairs Commission & Ministry of Education, South-Central University for Nationalities, Wuhan, China

ARTICLE INFO

Article history:
Received 14 October 2008
Received in revised form 5 January 2009
Accepted 14 January 2009
Available online 21 January 2009

Keywords:
Fischer–Tropsch synthesis
Co/Al_2O_3
Calcium oxide

ABSTRACT

A series of calcium oxide promoted cobalt catalysts were prepared by incipient wetness impregnation. The influence of the calcium oxide on the dispersion, reducibility and cobalt particle size of the catalysts was studied by different techniques, including N_2 adsorption, X-ray diffraction, temperature-programmed reduction, temperature-programmed desorption and oxygen titration. It was found that calcium oxide improved the cobalt oxide reducibility, especially for the reduction of CoO to Co^0. Since the interaction between cobalt oxide and the calcium oxide promoted support was suppressed, larger Co_3O_4 particles were formed on the surface. The catalytic activity for Fischer–Tropsch synthesis was evaluated in a continuous stirred tank reactor (CSTR). A positive correlation was observed between CO conversion, C_5^+ selectivity and calcium oxide content. Furthermore, methane selectivity decreased with increasing calcium oxide content. These could be attributed to the enhanced reducibility that provides abundant active sites.

© 2009 Published by Elsevier B.V.

1. Introduction

Fischer–Tropsch synthesis (FTS) is an important gas-to-liquids (GTL) technology, which catalytically converts syngas to liquid fuels with no sulfur and aromatics content [1–3]. Cobalt based catalysts were widely used for FTS due to their high activity, high selectivity to linear paraffins, low water-gas shift activity and stability toward deactivation by water [4]. Some inorganic supports with high surface area such as silica and alumina have been used to increase the surface area of the cobalt. Alumina is of great interest for slurry phase processes such as in continuous slurry tank reactors since it has a high surface area, high resistance to abrasion and is relatively stable over a wide temperature range. However, formation of irreversible cobalt-aluminate during pretreatment and under reaction conditions decreased the catalytic activity due to loss of active cobalt metal for catalyzing the reaction [5,6]. For alumina, the metal oxide-support interactions are stronger than other supports such as titania and silica [7]. In order to suppress these interactions, noble metals such as ruthenium [8] and rhenium [9] have been used as promoters. Indeed, these promoters can increase the reducibility and activity to a certain extent. However, due to high prices, their industrial application is restricted. Thus, less expensive metal oxides have been investigated as promoters.

It is known that addition of some metal oxide promoters to cobalt catalysts could modify the support's texture, suppress the formation of cobalt-supported compounds and increase cobalt dispersion and reducibility. It has been reported that some metal oxides, including ZrO_2 [7,10], La_2O_3 [11], MnOx [12], ZnO [13] and MgO [14], had significant effects on cobalt catalysts for Fischer–Tropsch syntheses. Dias and Assaf [15] studied the effect of calcium oxide content and the order of addition on the catalytic properties of Ni/Al_2O_3 catalyst for CO_2-reforming to methane. It was found that when CaO was impregnated first followed by nickel on Al_2O_3 support, calcium aluminate was formed, which reduced the subsequent formation of nickel aluminate due to competition between nickel and calcium for interaction with alumina. Quincoces et al. [16] obtained similar results and found that CaO could also prevent carbon deposition on the Ni/Al_2O_3 catalysts. Recently, Andonova et al. [17] studied CaO modification on Al_2O_3 supported Mo and Ni–Mo catalysts for hydrodesulfurization (HDS). The modified support showed higher pore volumes, stronger mechanical strength and more resistance to coke formation and deactivation than pure alumina.

The impact of calcium on the performance of iron-based catalyst for Fischer–Tropsch synthesis has been reported recently [18]. However, information on CaO promotion to $Co/\gamma\text{-}Al_2O_3$ catalyst for Fischer–Tropsch synthesis is very limited. In the present work, Co/Al_2O_3 catalysts modified with CaO were prepared and characterized and the catalysts' activity and selectivity were investigated.

2. Experimental

2.1. Catalyst preparation

2.1.1. Co/Al_2O_3

Co/Al_2O_3 catalyst was prepared by incipient wetness impregnation. The support, $\gamma\text{-}Al_2O_3$, BET surface area 230 $m^2\,g^{-1}$, average particle size 0.4–0.6 mm, pore volume 0.40 $cm^3\,g^{-1}$, was first

* Corresponding author. Tel.: +86 2767843016; fax: +86 2767842752.
E-mail addresses: jinlinli@hotmail.com, lij@mail.scuec.edu.cn (J. Li).

1381-1169/$ – see front matter © 2009 Published by Elsevier B.V.
doi:10.1016/j.molcata.2009.01.022

calcined at 600 °C for 6 h. Cobalt nitrate [$Co(NO_3)_2{\cdot}6H_2O$] was dissolved in deionized water and impregnated into the support using two-steps incipient wetness to give a final catalyst with 15 wt% cobalt. After each impregnation, the catalyst was dried at 120 °C for 12 h. After the last impregnation and drying, the catalyst was calcined at 350 °C for 6 h.

2.1.2. Co/Al_2O_3–CaO

CaO-modified alumina-supported cobalt catalysts were prepared by sequential impregnation. Calcium oxide-modified support was prepared by impregnating γ-Al_2O_3 with calcium nitrate aqueous solution. The sample was dried at 120 °C for 6 h and calcined in air at 550 °C for 6 h. In order to decompose calcium nitrate completely, calcination temperature was set to 550 °C. Two samples with CaO contents of 0.5 and 1.0 wt% of support were prepared. Then, cobalt was impregnated into the calcium oxide-modified support to produce a catalyst with 15 wt% cobalt using the same procedure as in Section 2.1.1. The CaO-promoted catalysts were denoted as Co/Al_2O_3–*n*CaO, where *n* refers to wt% CaO in the support.

2.2. Catalyst characterization

2.2.1. BET measurement

The BET surface area, pore volume and pore size distribution were calculated from the corresponding nitrogen adsorption isotherms obtained at −196 °C in a Quantachrome Adsorb-1. Prior to the adsorption measurements the samples were out-gassed at 200 °C for 6 h under vacuum (5×10^{-7} Pa).

2.2.2. X-ray powder diffraction

X-ray diffraction patterns were determined by a Brukers-D8 diffractometer using mono-chromatized Cu Kα radiation (λ = 1.54056 Å) operated at 40 kV and 40 mA and collected by a Vantec-1 detector within a wide 2-theta angular range. The spectra were recorded from $2\theta = 10^\circ$ to 80° with 0.0167° step using a 0.2 s acquisition time per step. XRK 900 reactor chamber (Anton Paar) mounted on a goniometers was used for in situ investigations under different gas atmosphere. The sample temperature and reaction gas flow through the sample were reliably controlled and measured. The identification of the phases was made with the help of JCPDS files (joint committee on powder diffraction standards). The average crystallite size of Co_3O_4 was calculated according to Scherrer's equation and Co_3O_4 particle size was converted to cobalt metal particle size according to the formula below [19]:

$$d(Co^0) = 0.75d(Co_3O_4)$$

For in situ XRD measurement, the gas flow (H_2 and 10%H_2/Ar) was fixed at 30 ml (NTP)/min and the heating rate at 10 °C/min. At first, the catalyst was purged with N_2 at 150 °C for 1 h to flush away water and impurities. After cooling down to room temperature, the reduction gas was switched to the sample cell. For the pure hydrogen condition, the temperature was increased from room temperature to 450 °C, after which it was followed by several scans with a waiting period of 1 h between scans, while for 10%H_2/Ar reduction condition, the temperature was increased from room temperature to 800 °C.

2.2.3. Temperature programmed reduction (TPR)

Temperature programmed reduction experiments were carried out on a Zeton Altamira AMI-200 unit. Calcined catalysts were first flushed with argon at 150 °C for 1 h and then cooled down to 50 °C. Subsequently, the sample was heated to 800 °C at a heating ramp rate of 10 °C/min under 10%H_2/Ar mixture at 30 ml/min. TCD signals were recorded from 50 °C to 800 °C.

2.2.4. Temperature programmed desorption (TPD) and O_2 titration

To investigate the cobalt dispersion and percentage reduction, hydrogen temperature programmed desorption followed by re-oxidation measurements were performed on a Zeton Altamira AMI-200 unit. The catalysts were reduced in flowing H_2 at 450 °C for 12 h with a temperature ramp rate of 10 °C/min. The samples were then cooled to 100 °C under hydrogen gas flow and purged with argon at 100 °C for 1 h to remove physisorbed species prior to increasing the temperature slowly to 450 °C. At that temperature, the catalyst was held under flowing argon to desorb the remaining chemisorbed hydrogen until the TCD signal returned to the baseline. The TPD spectrum was integrated and the amount of desorbed hydrogen was determined by comparing the mean areas of calibrated hydrogen pulses.

The reduced catalyst was re-oxidized at 450 °C by purging with oxygen pulses, until no further consumption of O_2 was detected by the thermal conductivity detector located downstream. High purity helium acted as reference gas for TCD. The extent of reduction was calculated assuming stoichiometric re-oxidation of Co to Co_3O_4. All flow rates were set to 30 ml/min. The uncorrected dispersions are based on the assumption of complete reduction. The formula for the calculation has been shown in previous studies [7].

2.3. Fischer–Tropsch synthesis

Fischer–Tropsch synthesis was performed in a 1 L slurry-phase continuously stirred tank reactor (CSTR). Prior to the reactor test, ca. 6.0 g catalyst was externally reduced at 450 °C under atmospheric pressure of H_2 with a flow rate of 6 SL/h g for 10 h. The reduced catalyst was transferred to the CSTR loading with 300 g liquid wax medium. The catalyst was reduced again at 280 °C for 14 h in a H_2 flow of 30 NL/h in situ. After reduction the reactor temperature was decreased to 180 °C, the syngas (molar ratio of $H_2/CO = 2.0$, GHSV = 3 SL/h g) was introduced and the pressure was increased to 10 bar. The reaction temperature was then increased to 230 °C and the effluent gaseous products were taken at 2 h intervals and analyzed using on-line Agilent GC3000 with a TCD detector.

3. Results and discussion

3.1. Nitrogen adsorption measurement

The surface area, average pore diameter and pore volume for the catalysts, calculated from the nitrogen adsorption–desorption isotherms, are shown in Table 1. These values as well as pore size distribution (not shown here) are similar for all the catalysts suggesting that calcium oxide addition did not alter the physical property of the support.

3.2. X-ray diffraction

XRD patterns of the catalysts are presented in Fig. 1. Only crystalline Co_3O_4 phase and γ-Al_2O_3 are observed after calcination. No peaks of CaO or other calcium compounds are detected, indicating that CaO was dispersed on the support as a monolayer or formed spinel-like or tridymite-like structure with no detectable interaction between the promoter and support [20]. The average crystalline size of Co_3O_4, calculated according to Scherrer's equation from the line broadening of (3 1 1) diffraction peak, are shown in Table 1. The average Co_3O_4 particle size increased with the CaO loading. It is noted that the average diameter is larger than the support pore diameter so that some large Co_3O_4 were located on the external surface of the support.

Table 1
Surface area, pore volume and average pore diameter.

Catalyst	Surface area (m^2/g)	Average pore diameter (nm)	Pore volume (cm^3/g)	Co_3O_4 diameter[a] (nm)
Co/Al_2O_3	131.5	9.2	0.41	9.5
Co/Al_2O_3–0.5CaO	135.0	9.1	0.42	12.6
Co/Al_2O_3–1.0CaO	135.5	9.4	0.42	13.1

[a] Average Co_3O_4 particle diameter obtained from XRD data.

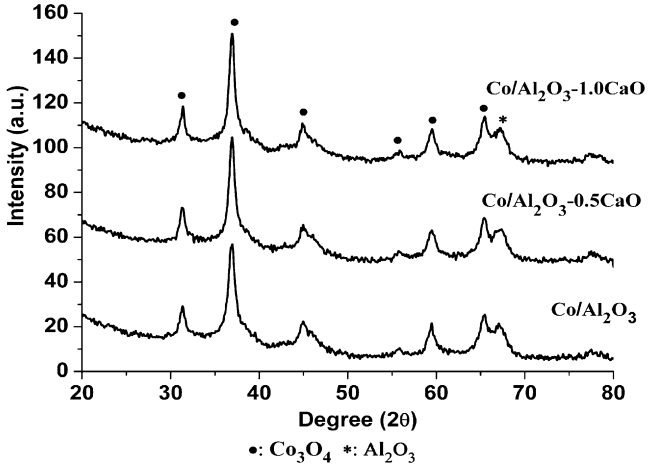

Fig. 1. X-ray diffraction patterns for unpromoted and promoted, calcined Co/Al_2O_3 catalysts.

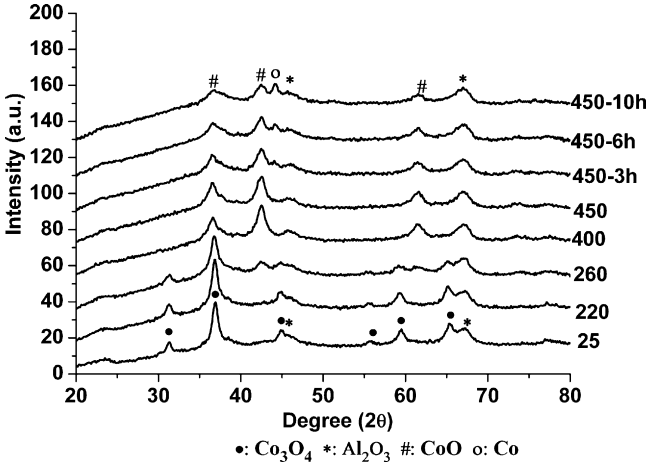

Fig. 3. In situ X-ray diffraction patterns of Co/Al_2O_3 catalyst reduced in H_2.

The in situ XRD patterns of the Co/Al_2O_3 catalyst reduced by 10%H_2/Ar are shown in Fig. 2. As can be seen, reduction of Co/Al_2O_3 proceeded in two steps: Co_3O_4 to CoO and CoO to Co metal. The first step was completed at about 400 °C, as evidenced by the shift of the oxide diffraction of 36.9° (Co_3O_4) to 36.5° (CoO) and appearance of the 42.5° and 61.6° lines. The intensity of these lines decreased with increasing temperature as CoO was gradually transformed to metallic cobalt. At 700 °C, CoO has completely been reduced. Figs. 3–5 display the XRD patterns of Co/Al_2O_3, Co/Al_2O_3–0.5CaO and Co/Al_2O_3–1.0CaO catalysts measured in situ during the reduction under pure hydrogen. All of the Co_3O_4 were reduced to CoO whereas the extent of further reduction to the metal phases varied depending on the sample. In Co/Al_2O_3 catalyst, Co_3O_4 was transformed completely to CoO at about 400 °C, then started to be further reduced to metallic cobalt. However, the CoO lines were clearly visible even after 10 h at 450 °C. It is thus suggested that some CoO still remained unreduced during the cobalt activation for the Fischer–Tropsch

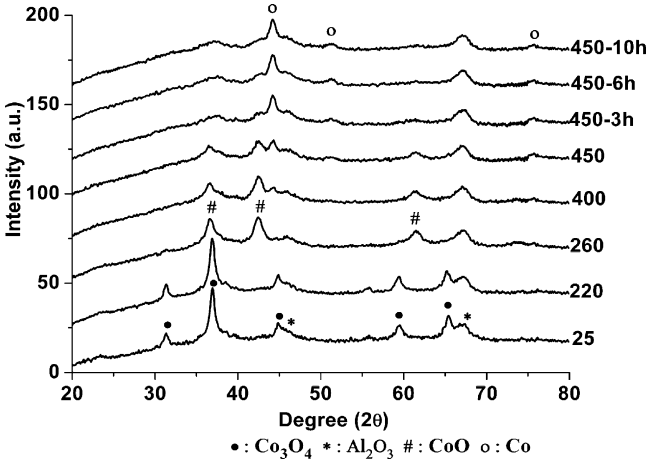

Fig. 4. In situ X-ray diffraction patterns of Co/Al_2O_3–0.5CaO catalyst reduced in H_2.

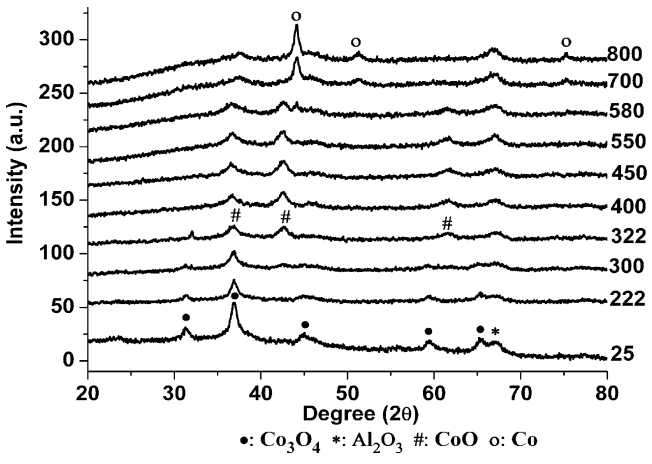

Fig. 2. In situ X-ray diffraction patterns of Co/Al_2O_3 catalyst reduced in H_2/Ar.

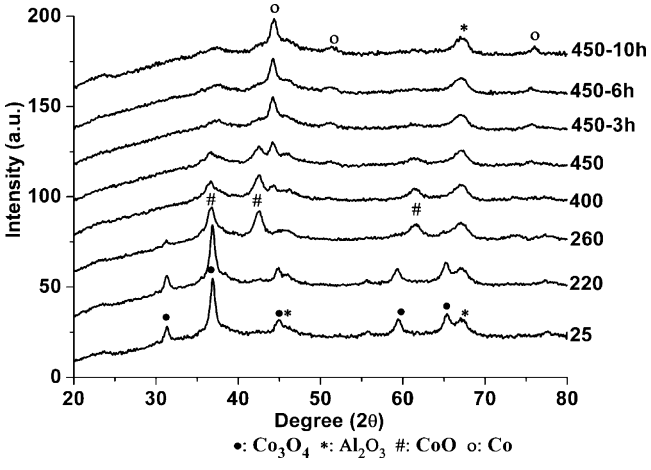

Fig. 5. In situ X-ray diffraction patterns of Co/Al_2O_3–1.0CaO catalyst reduced in H_2.

Table 2
H_2-temperature programmed desorption and O_2 pulse re-oxidation results for catalysts.

Sample	H_2 desorbed (μmol/g)	d_{uncorr}[a] (%)	D_{uncorr}[b] (nm)	O_2 uptake (μmol/g)	d_{corr}[c] (%)	Reducibility (%)	D_{corr}[d] (nm)	D[e] (nm)
Co/Al_2O_3	164.2	12.66	6.0	725.2	29.8	42.5	2.6	7.1
Co/Al_2O_3–0.5CaO	160.3	12.45	8.4	745.8	28.5	43.7	3.7	9.5
Co/Al_2O_3–1.0CaO	158.5	12.27	9.4	810.1	25.8	47.5	4.5	9.8

[a] The uncorrected catalyst dispersion.
[b] The uncorrected cobalt metal cluster diameter.
[c] The corrected catalyst dispersion.
[d] The corrected cobalt metal cluster diameter.
[e] Cobalt particle size calculated from XRD measurement, using $d(Co^0) = 0.75d(Co_3O_4)$.

synthesis in this work. In contrast to Co/Al_2O_3, Co/Al_2O_3–0.5CaO exhibited higher extent of reduction. Co_3O_4 was transformed to CoO at a lower temperature of 260 °C and CoO diffraction peaks almost disappeared after 10 h reduction. Co/Al_2O_3–1.0CaO catalyst showed similar behavior to that of Co/Al_2O_3–0.5CaO, however, the relative intensity of the reduced cobalt was higher than the other two. It is well known that cobalt ions interact with alumina support to form cobalt aluminate which is difficult to reduce. The interaction between the cobalt ions and the support is stronger when it is surrounded by more Al^{3+} ions and become harder to reduce [21]. For calcium oxide promoted catalysts, calcium oxide was highly dispersed on the support surface reducing the contact between cobalt ions and support which decreases the number of Al^{3+} ions surrounding the cobalt ions so that metal support interaction became increasing weaker with higher calcium oxide content. As a consequence, the reducibility of alumina supported cobalt catalysts increased significantly with calcium oxide promotion. In addition, calcium oxides promoted catalysts have a tendency to form larger Co_3O_4 particle than calcium oxide-free catalyst. Figs. 3–5 showed that relative intensity of Co was higher for samples with larger oxide particles, the reduction of which increases with increased particle size. The same conclusion was obtained by Castner et al. [22] from their study of hydrogen reduction of two Co catalysts supported on silica with different pore sizes. They found that the difficulty of the reduction of CoO to Co increased with decreasing pore size of the silica and hence decreasing cobalt oxide particle size.

3.3. H_2-temperature programmed reduction

TPR profiles of the catalysts are displayed in Fig. 6. Two major peaks for Co/Al_2O_3 were observed at temperature ranges of 280–380 °C and 380–750 °C, respectively. Combined with the in situ XRD patterns under reduction by 10%H_2/Ar, the first peak could be assigned to the reduction of Co_3O_4 to CoO. Jacobs et al. [23] also showed that Co_3O_4 underwent virtually 100% transition to CoO prior to the formation of Co below 400 °C. The second peak is ascribed to the subsequent reduction of CoO to Co^0, however, the existence of a cobalt aluminate could not be excluded. Besides these two main reduction peaks, a small peak appeared at about 260 °C. This peak could be attributed to the reduction of residual cobalt nitrate [4,19], which decomposed completely above 400 °C [24]. There were also two major peaks for the Co/Al_2O_3–0.5CaO located at 250–370 °C and 370–750 °C. It would appear that the broad peak shifted about 40 °C to lower temperature than for the unpromoted catalyst, indicating calcium oxide promotion caused changes in reduction behavior of the Co catalysts. The relative contribution of the species reduced at lower temperatures can be ascribed to the lower strength of interaction between Co^{2+} and alumina support, as observed in the in situ XRD data. Co/Al_2O_3–1.0CaO catalyst showed a similar second step reduction peak with the first step reduction peak occurring at a slightly higher temperature. It is noted that CaO-promoted catalysts facilitated the nitrate reduction. For the Co/Al_2O_3–0.5CaO catalyst, the peak shifted to lower temperature and for Co/Al_2O_3–1.0CaO catalyst, the nitrate peak almost disappeared completely. The reason for this is not clear at the moment.

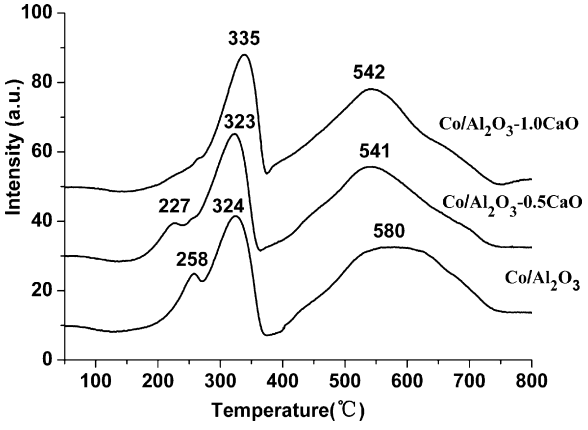

Fig. 6. TPR profiles of unpromoted and promoted, calcined catalysts.

3.4. H_2-temperature programmed desorption and O_2 pulse re-oxidation

Table 2 presents the H_2-temperature programmed desorption and O_2 pulse re-oxidation data. It is clearly seen that calcium oxide affected the dispersion, reducibility and cobalt particle size. Both the catalyst's reducibility and cobalt particle size increase and dispersion decreases with calcium oxide addition, which is in agreement with the in situ XRD results. Cobalt particle size calculated H_2-chemisorption is smaller compared with XRD results. The main reasons are probably that XRD measurement missed the small particles and crystallite sizes obtained from XRD patterns could overestimate the sizes of crystallite particles [25].

3.5. Fischer–Tropsch synthesis

Results of the Fischer–Tropsch synthesis tests are displayed in Table 3. CO conversion and selectivity to higher hydrocarbon increase with increasing calcium oxide content. However, methane selectivity and light weight hydrocarbons (C_2–C_4) show an opposite trend to C_5^+ selectivity.

It is well known that reducibility plays an important role in determining catalyst activity and selectivity. In this study, it is shown that calcium oxide facilitated the cobalt oxide reduc-

Table 3
FTS reaction CO conversion and product distribution.

Catalysts	CO conversion (%)	Hydrocarbon selectivity (%)				
		CH_4	C_2	C_3	C_4	C_5+
Co/Al_2O_3	35.31	12.18	1.19	4.05	4.82	77.75
Co/Al_2O_3–0.5CaO	37.93	9.88	0.99	3.55	4.29	81.30
Co/Al_2O_3–1.0CaO	39.67	8.61	1.04	3.12	3.70	83.54

tion, especially for the reduction step of CoO to Co. During Fischer–Tropsch synthesis, it was known that high reducibility provided more cobalt active sites and hence, increased the catalytic activity [2,6,26–29]. Thus, the increase in catalyst activity appeared to be mainly due to the increased reducibility and formation of more cobalt active sites.

Cobalt catalyst shows a strong tendency for secondary reactions involving re-adsorption and incorporation of reactive compounds, such as ethene and propene, into growing chains. If these smaller products were re-adsorbed and acted as chain initiators, the selectivity of the C_5^+ fraction will increase. The calcium oxide modified catalysts with higher reducibility provide more cobalt surface sites than the calcium oxide-free catalyst. Thus, higher re-adsorption of the α-olefins occurs. The re-adsorbed olefins participate in the chain-growing process favoring the formation of high molecular weight products. Methane selectivity is up to 12.18% for unpromoted catalyst. With calcium oxide addition, the methane selectivity decreased significantly to 9.88% for Co/Al_2O_3–0.5CaO and 8.61% for Co/Al_2O_3–1.0CaO catalyst. High methane selectivity has been reported for low reducibility and high dispersion [30] attributed to the presence of unreduced cobalt oxides catalyzing the WGS reaction, thus increasing the effective H_2/CO ratio at the catalyst surface. The local increase of the H_2/CO ratio near the surface Co^0 sites would favor hydrogenation of the adsorbed species leading to higher methane selectivity.

Tables 2 and 3 show that C_5^+ selectivity increased along with cobalt particle size. Co/Al_2O_3–1.0CaO (4.5 nm) and Co/Al_2O_3–0.5CaO (3.7 nm), which have larger cobalt particle than Co/Al_2O_3 (2.6 nm), have higher C_5^+ and lower methane selectivities. It has been shown that the steric hindrance for dissociative adsorption of CO and olefin monomer and addition of this monomer to the growing chain was lower on large cobalt particle [31]. On the other hand, the chain propagation and growth probability on the surface of the larger cobalt particle is higher than that of smaller ones. Bezemer et al. [32] also obtained similar result that C_5^+ selectivity increased with increasing cobalt particle size. However, they ascribed that to non-classical structure sensitivity in combination with CO-induced surface reconstruction. In those works, inert material carbon nanotube and carbon nanofiber were used as support to avoid support influence to product selectivity [31,32]. As calcium oxide addition does not significantly change the support property, the product selectivity could be ascribed to a particle size effect.

4. Conclusion

A series of unpromoted and CaO-promoted Co/Al_2O_3 catalysts were studied using different characterization techniques. In situ XRD and TPR results show that calcium oxide suppresses the interaction between cobalt oxide and support resulting in increased cobalt reducibility, more cobalt active sites and larger cobalt particle size. The effect of calcium oxide on the Fischer–Tropsch synthesis activity and selectivity investigated in a continuously stirred tank reactor shows that the activity and C_5^+ selectivity increased and methane selectivity decreased with increasing calcium oxide content attributed to the increased reducibility and cobalt particle size.

Acknowledgement

Financial support from National Natural Science Foundation of China (Grant Nos: 20590360 and 20773166) are gratefully acknowledged.

References

[1] A.Y. Khodaov, W. Chu, P. Fongarland, Chem. Rev. 107 (2007) 1692–1744.
[2] A. Martinez, C. Lopez, F. Marquez, I. Diaz, J. Catal. 220 (2003) 486–499.
[3] M.E. Dry, Catal. Today 71 (2002) 227–241.
[4] Ø. Borg, S. Eri, E.A. Blekkan, S. Stosater, H. Wigum, E. Rytter, A. Holmen, J. Catal. 248 (2007) 89–100.
[5] S.A. Hosseini, A. Taeb, F. Feyzi, F. Yaripour, Catal. Commun. 5 (2004) 137–143.
[6] J.L. Zhang, J.G. Chen, J. Ren, Y.H. Sun, Appl. Catal. A: Gen. 243 (2003) 121–133.
[7] G. Jacobs, T.K. Das, Y.Q. Zhang, J.L. Li, G. Racoillet, B.H. Davis, Appl. Catal. A: Gen. 233 (2002) 263–281.
[8] S.A. Hosseini, A. Taeb, F. Feyzi, Catal. Commun. 6 (2005) 233–240.
[9] T.K. Das, G. Jacobs, P.M. Patterson, W.A. Conner, J.L. Li, B.H. Davis, Fuel 82 (2003) 805–815.
[10] B. Jongsomjit, J. Panpranot, J.G. Goodwin Jr., J. Catal. 215 (2003) 66–77.
[11] J.S. Ledford, M. Houalla, A. Proctor, D.M. Hercules, L. Petrakis, J. Phys. Chem. 93 (1989) 6770–6777.
[12] M. Nurunnabi, K. Murata, K. Okabe, M. Inaba, I. Takahara, Catal. Commun. 8 (2007) 1531–1537.
[13] G.A. El-Shobaky, G.A. Fagal, M. Mokhtar, Appl. Catal. A: Gen. 155 (1997) 167–178.
[14] Y.H. Zhang, H.F. Xiong, K.Y. Liew, J.L. Li, J. Mol. Catal. A: Chem. 237 (2005) 172–181.
[15] J.A.C. Dias, J.M. Assaf, Catal. Today 85 (2003) 59–68.
[16] C.E. Quincoces, S. Dicundo, A.M. Alvarez, M.G. Gonzalez, Mater. Lett. 50 (2001) 21–27.
[17] S. Andonova, Ch. Vladov, B. Pawelec, I. Shtereva, G. Tyuliev, S. Damyanova, L. Petrov, Appl. Catal. A: Gen. 328 (2007) 201–209.
[18] Z.C. Tao, Y. Yang, C.H. Zhang, T.Z. Li, J.H. Wang, H.J. Wan, H.W. Xiang, Y.W. Li, Catal. Commun. 7 (2006) 1061–1066.
[19] A.M. Hilmen, D. Schanke, K.F. Hanssen, A. Holmen, Appl. Catal. A: Gen. 186 (1999) 169–188.
[20] T. Horiuchi, H. Hidaka, T. Fukui, Y. Kubo, M. Horio, K. Suzuki, T. Mori, Appl. Catal. A: Gen. 167 (1998) 195–202.
[21] P. Arnoldy, J.A. Moulijn, J. Catal. 93 (1985) 38–54.
[22] D.G. Castner, P.R. Watson, I.Y. Chan, J. Phys. Chem. 94 (1990) 819–828.
[23] G. Jacobs, Y.Y. Ji, B.H. Davis, D. Cronauer, A.J. Kropf, C.L. Maeshall, Appl. Catal. A: Gen. 333 (2007) 177–191.
[24] Ø. Borg, E.A. Blekkan, S. Eri, D. Akporiaye, B. Vigerust, E. Rytter, A. Holmen, Top. Catal. 45 (2007) 39–43.
[25] P. Ganesan, H.K. Kuo, A. Saavedra, R.J. De Angelies, J. Catal. 52 (1978) 310–320.
[26] A.R. Belamble, R. Oukaci, J.G. Goodwin Jr., J. Catal. 166 (1997) 8–15.
[27] J.L. Li, N.J. Coville, Appl. Catal. A: Gen. 181 (1999) 201–208.
[28] Y. Wang, M. Noguchi, Y. Takahashi, Y. Ohtsuka, Catal. Today 68 (2001) 3–9.
[29] A.Y. Khodakov, R. Bechara, A. Griboval-Constant, Stud. Surf. Sci. Catal. 142 (2002) 1133–1140.
[30] R.C. Reuel, C.H. Bartholomew, J. Catal. 85 (1984) 63–77.
[31] A. Tavasoli, R.M.M. Abbaslou, M. Trepanier, A.K. Dalai, Appl. Catal. A: Gen. 345 (2008) 134–142.
[32] G.L. Bezemer, J.H. Bitter, H.P.C.E. Kuipers, H. Oosterbeek, J.E. Holewijn, X.D. Xu, F. Kapteijn, A.J. van Dillen, K.P. de Jong, J. Am. Chem. Soc. 128 (2006) 3956–3964.